Supporting Information

Structure of nanocrystalline, partially disordered $MoS_{2+\delta}$ derived from HRTEM – an abundant material for efficient HER catalysis

Emanuel Ronge [1], Sonja Hildebrandt [1], Marie-Luise Grutza [2], Helmut Klein [3], Philipp Kurz [2,*] and Christian Jooss [1,4,*]

[1] Institute of Materials Physics University of Goettingen, Friedrich-Hund-Platz 1, 37077 Goettingen, Germany; eronge@gwdg.de (E.R.); s.hildebrandt01@stud.uni-goettingen.de (S.H.); cjooss@gwdg.de (C.J.);
[2] Institute for Inorganic and Analytical Chemistry and Freiburg Material Research Center (FMF), University of Freiburg, Albertstraße 21, 79104 Freiburg, Germany; marie-luise.grutza@ac.uni-freiburg.de (M.L.G.); philipp.kurz@ac.uni-freiburg.de (P.K))
[3] GZG Crystallography University of Goettingen, Goldschmidtstr. 1, 37077 Göttingen, Germany; hklein@uni-goettingen.de (H.K.)
[4] International Center for Advanced Studies of Energy Conversion (ICASEC), Georg-August-University, D-37077 Göttingen, Germany; cjooss@gwdg.de (C.J.)
* Correspondence: cjooss@gwdg.de (C.J.); philipp.kurz@ac.uni-freiburg.de (P.K.)

1. XRD

Table S1. Comparison of the experimental (XRD) d_{hkl} from figure 2 for $MoS_{2+\delta}$ with the literature values for the most intense XRD reflections of MoS_2[a)] and selected area electron diffraction (SAD) pattern from Figure 3.

XRD	SAD	XRD	SAD	*Literature*[a)]	
$MoS_{2.6}$	$MoS_{2.6}$	$MoS_{3.4}$	$MoS_{3.4}$	MoS_2	*(hkl)*
Å	*Å*	*Å*	*Å*	*Å*	
7.59		8.19			
6.29					
6.08				6.15	002
	4.51			2.74	100
	3.18				
2.70		2.63		2.67	101
2.51				2.50	102
2.15	2.28	2.14	2.35	2.28	103
1.89		1.87	1.98	1.83	105
1.62	1.46	1.62	1.52	1.57	110
	1.04		1.089		

[a)] Structure model of Wildervanck et al was used [1].

1.1 Rietveld refinement

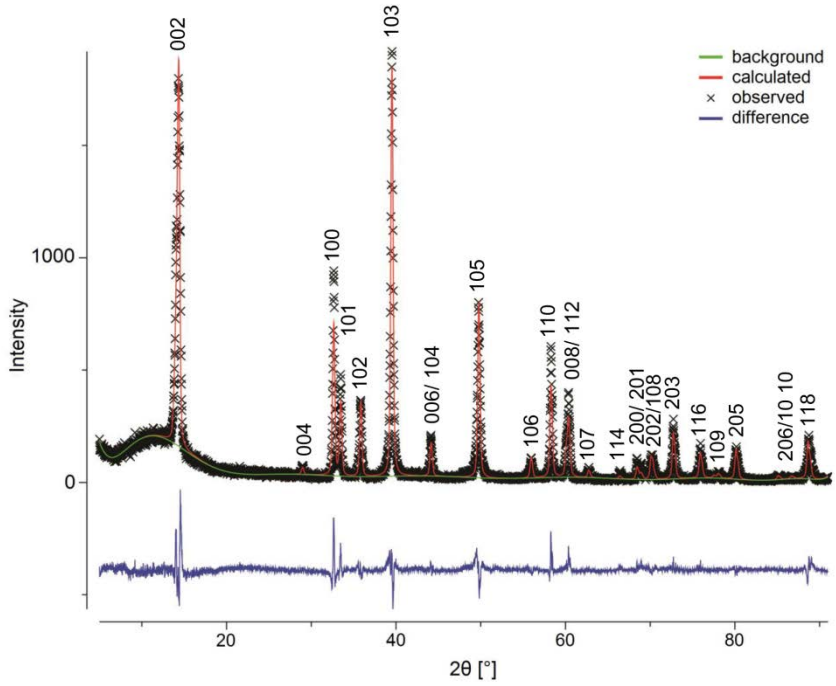

Figure S1. Plot of the Rietveld refinement of MoS_2.

Table S2. Goodness parameters and correction factor for the texture.

χ^2	R_{wp}	G
2.857	0.1847	1.005 ± 0.003

Table S3. Refined lattice parameters and atom positions of MoS_2.

a	b	c
Å	*Å*	*Å*
3.16354 ± 0.00014	3.16354 ± 0.00014	12.3086 ± 0.0008

Atom	x	y	z
Mo	0.3333	0.6667	0.2500
S	0.3333	0.6667	0.6225 ± 0.0003

2. TEM

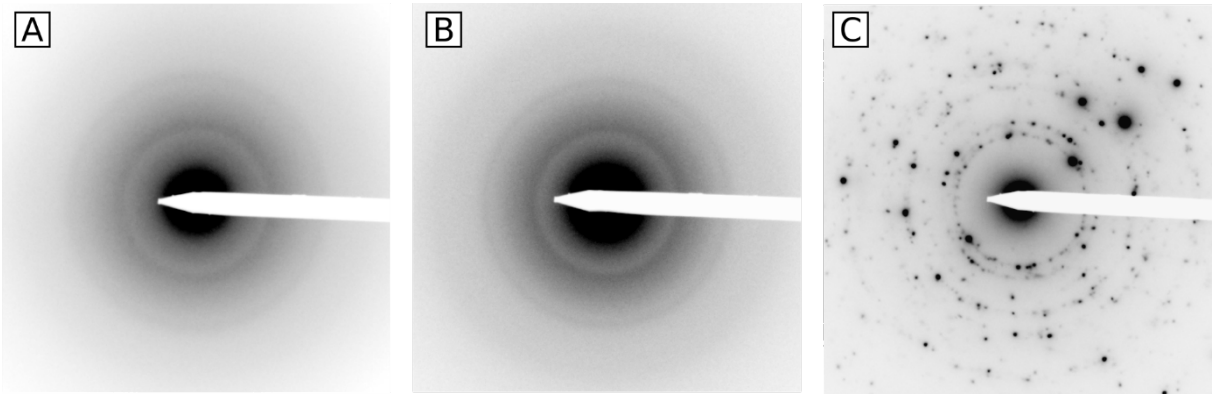

Figure S2. Selected area electron diffraction (SAD) patterns of A: $MoS_{2.6}$; B: $MoS_{3.4}$; C: MoS_2.

In Table S4 the most intense lattice reflections of MoS_2 from the structure of Wildervanck et al. [28] are compared to experimental selected area electron diffraction (SAD) results of MoS_2, $MoS_{2.6}$ and $MoS_{3.4}$ after creating diffracted intensity profiles via circular integration as shown in Figure 3. There, the experimental numbers give the peak positions and the grey shadow represents the peak width. For MoS_2 every lattice reflection with $F^2 > 10^6$ can be assigned. Some of the reflections are hidden in the flanks in the intensity profile (Figure 3) due to their lower intensity but are visible in the diffraction pattern in Figure S3. The (004) reflection is probably missing due to its low structure factor and the (002) reflection is missing for all samples due to its overlap with the zero beam.
The SAD intensity profiles of $MoS_{2.6}$ and $MoS_{3.4}$ is similar to the profile of MoS_2, but their shape is significantly broadened. Thus, most important MoS_2 reflexes can be assigned to the SAD data of the partially disordered systems. However, in the range of 1.29 Å and 1.15 Å no broadened reflexes are visible for $MoS_{2.6}$ and $MoS_{3.4}$, in contrast to the expected diffraction maxima from the literature as well as the experimental MoS_2 data. This could indicate an increase of disorder for these lattice planes. In addition, the (004) reflection can be assigned to the $MoS_{2.6}$ data. The increased disorder in c direction could explain why these reflections are visible compared to MoS_2. This is supported by XRD (main text Figure 2) which show in general a lower order compared to MoS_2 but a sharp c-direction compared to $MoS_{3.4}$.

Table S4. Overview on the most intense lattice reflections ($F^2 > 10^6$ and d > 1 Å) in electron diffraction of MoS_2 compared with experimental SAD data for MoS_2, $MoS_{2.6}$ and $MoS_{3.4}$ from Figure S3 and main text Figure 3. The structure model of Wildervanck et al. [28] and the atomic scattering factor from Colliex et al. [29] were used to calculate the structure factor F.

Literature [28,29]					Experimental		
MoS_2					MoS_2	$MoS_{2.6}$	$MoS_{3.4}$
d [Å]	(h	k	l)	F^2	d [Å]	d [Å]	d [Å]
6.147	0	0	$\bar{2}$	$4.61 \cdot 10^8$	Overlapp with zero beam		
3.074	0	0	$\bar{4}$	$4.85 \cdot 10^6$	-	3.18	-
2.737	$\bar{1}$ $\bar{1}$	0 1	0 0	$1.40 \cdot 10^9$	Could be hidden in flank		
2.671	$\bar{1}$	0	$\bar{1}$	$6.98 \cdot 10^7$			
2.500	$\bar{1}$ $\bar{1}$	0 1	$\bar{2}$ $\bar{2}$	$7.01 \cdot 10^8$	2.52	2.31	2.35
2.276	$\bar{1}$	0	$\bar{3}$	$5.62 \cdot 10^9$			
2.049	0	0	$\bar{6}$	$2.86 \cdot 10^8$	2.13		
2.044	$\bar{1}$	0	$\bar{4}$	$7.43 \cdot 10^6$			1.99
1.830	$\bar{1}$	0	$\bar{5}$	$6.66 \cdot 10^9$	Hidden in flank		
1.640	$\bar{1}$ $\bar{1}$	0 1	$\bar{6}$ $\bar{6}$	$4.36 \cdot 10^8$	1.72		
1.580	$\bar{2}$ $\bar{1}$	1 $\bar{1}$	0 0	$5.77 \cdot 10^9$	Hidden in Flank		
1.537	0	0	$\bar{8}$	$1.80 \cdot 10^9$			
1.530	$\bar{2}$ $\bar{1}$	1 $\bar{1}$	$\bar{2}$ $\bar{2}$	$2.88 \cdot 10^9$			1.52
1.478	$\bar{1}$	0	$\bar{7}$	$2.47 \cdot 10^8$	1.47	1.45	
1.405	$\bar{2}$	1	$\bar{4}$	$3.06 \cdot 10^7$	1.42		
1.368	$\bar{2}$ $\bar{2}$	0 2	0 0	$1.46 \cdot 10^9$			
1.360	$\bar{2}$	0	$\bar{1}$	$7.28 \cdot 10^7$	Hidden in flank		
1.340	$\bar{1}$	0	$\bar{8}$	$2.75 \cdot 10^9$			
1.336	$\bar{2}$	0	$\bar{2}$	$7.29 \cdot 10^8$			
1.298	$\bar{2}$	0	$\bar{3}$	$5.84 \cdot 10^9$			
1.251	$\bar{2}$ $\bar{1}$	1 $\bar{1}$	$\bar{6}$ $\bar{6}$	$1.79 \cdot 10^9$	1.27		
1.250	$\bar{2}$ $\bar{2}$	0 2	$\bar{4}$ $\bar{4}$	$7.71 \cdot 10^6$			
1.222	$\bar{1}$ $\bar{1}$	0 1	$\bar{9}$ $\bar{9}$	$5.87 \cdot 10^6$			
1.196	$\bar{2}$	0	$\bar{5}$	$6.93 \cdot 10^9$	1.20		
1.138	$\bar{2}$	0	$\bar{6}$	$4.53 \cdot 10^8$	Hidden in flank		
1.102	$\bar{2}$	1	$\bar{8}$	$1.13 \cdot 10^{10}$	1.11		
1.079	$\bar{2}$	0	$\bar{7}$	$2.57 \cdot 10^8$	1.06		1.089
1.034	$\bar{3}$ $\bar{2}$	1 $\bar{1}$	0 0	$3.02 \cdot 10^9$		1.04	
1.031	$\bar{3}$ $\bar{2}$	1 $\bar{1}$	$\bar{1}$ $\bar{1}$	$1.51 \cdot 10^8$			
1.022	$\bar{2}$	0	$\bar{8}$	$2.86 \cdot 10^9$			
1.020	$\bar{3}$	1	$\bar{2}$	$1.51 \cdot 10^9$			
1.003	$\bar{3}$	1	$\bar{3}$	$1.21 \cdot 10^{10}$			

Table S5. Result from the FFT analysis of HRTEM images of $MoS_{2+\delta}$ visible in Figure S3.

	$d_{\{100\}}$ Å	$d_{\{001\}}$ Å
$MoS_{2.6}$	2.70 ± 0.19	12.4 ± 0.2
	2.60 ± 0.03	12.6 ± 0.3
	2.66 ± 0.19	13.4 ± 0.2
	2.45 ± 0.18	14.1 ± 0.3
	2.56 ± 0.05	13.3 ± 0.3
		13.3 ± 0.3
		11.2 ± 0.2
$MoS_{3.4}$	2.75 ± 0.05	13.2 ± 0.4
	2.71 ± 0.11	15.9 ± 0.6
	2.61 ± 0.09	11.8 ± 0.5
	2.79 ± 0.03	14.3 ± 0.7
	2.73 ± 0.11	12.5 ± 0.7

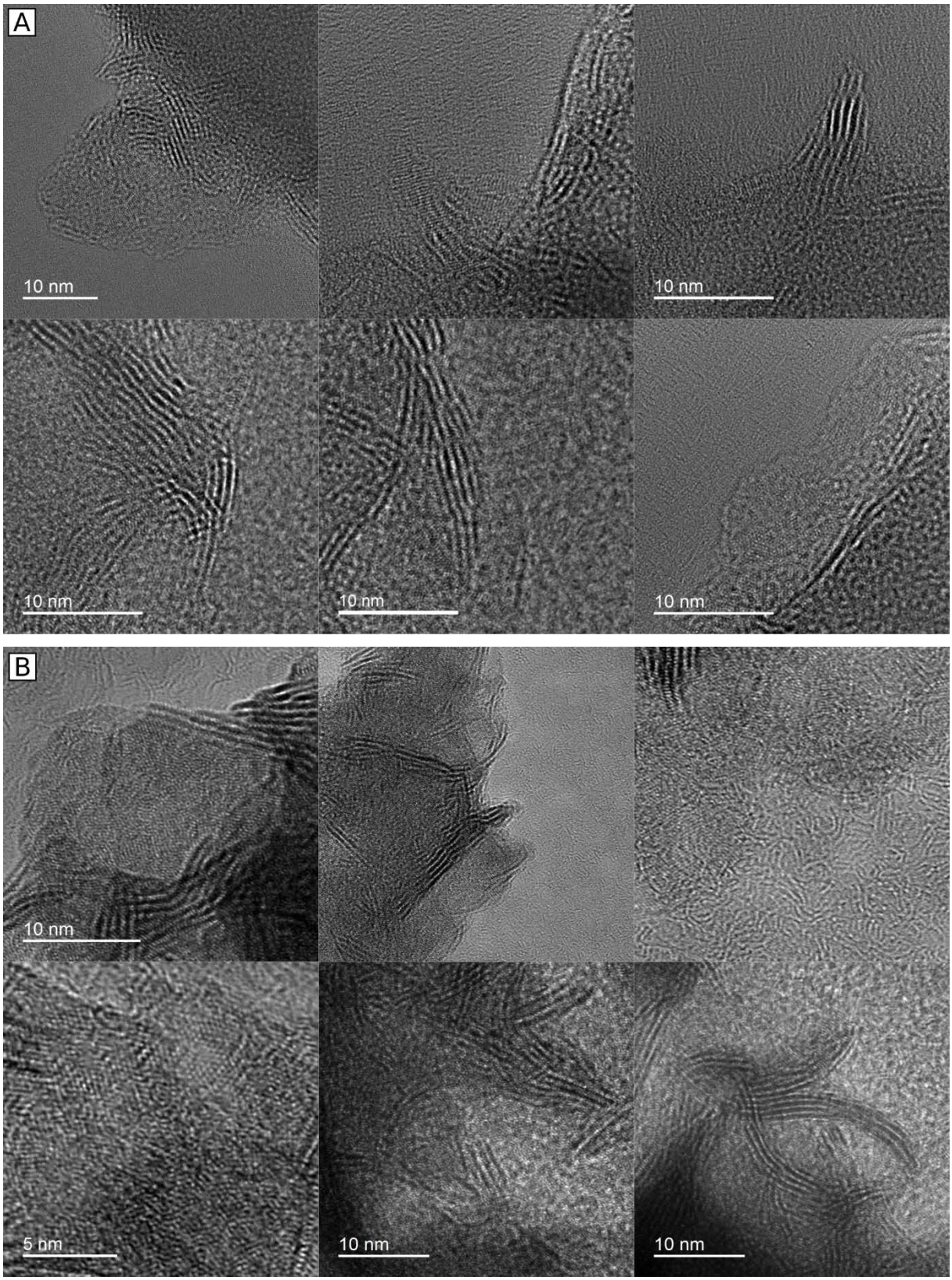

Figure S3. HRTEM images of A: $MoS_{2.6}$ and B: $MoS_{3.4}$ used for the lattice parameter analysis in Table S5.

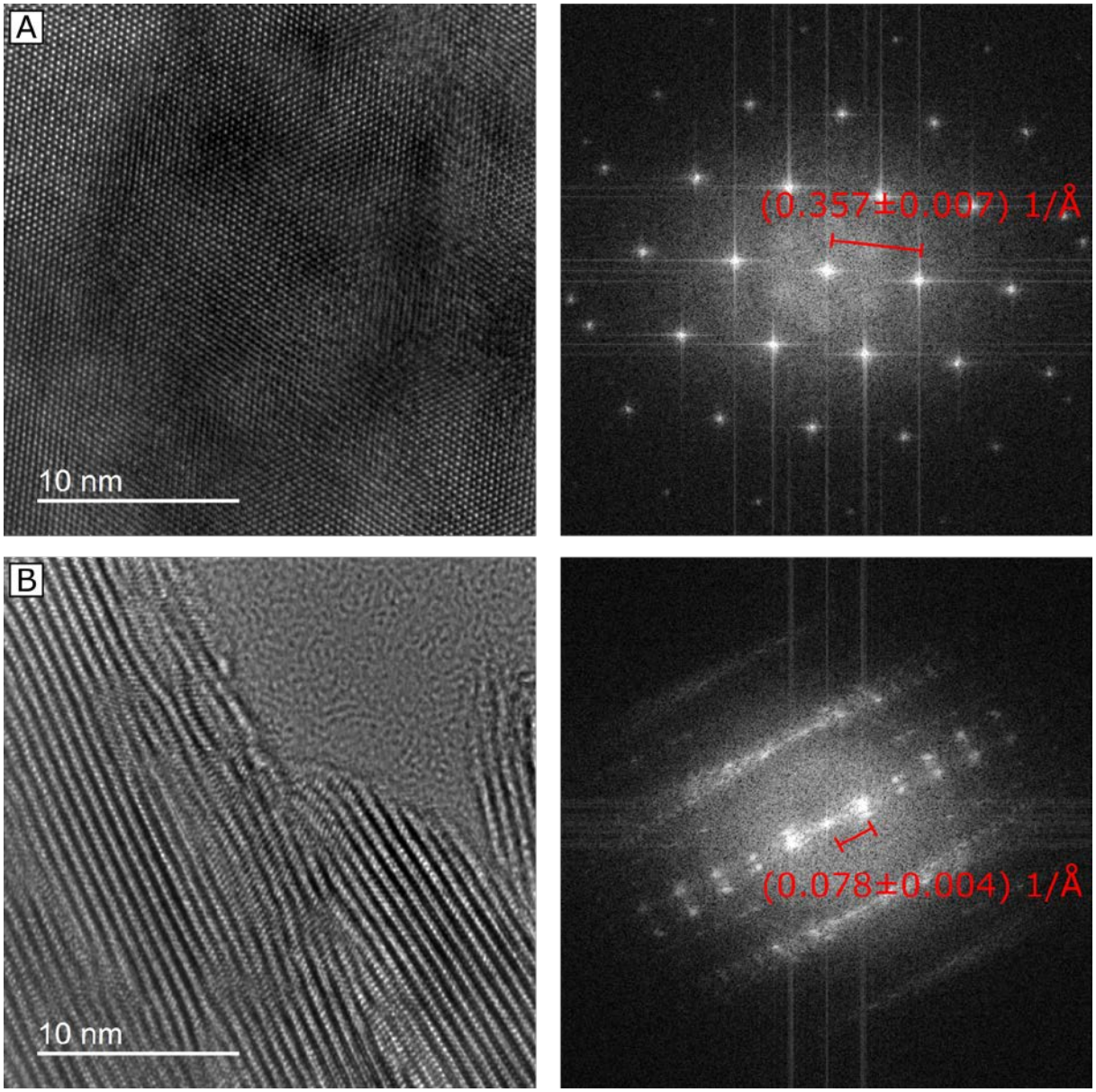

Figure S4. Representative HRTEM images of MoS_2 and their FFTs (in red the measured mean lattice parameter). A: in-plane ($1/\bar{d}$=0.357±0.007) 1/Å → $\bar{d}_{(100)}$=(2.80±0.06) Å); B: out of plane ($1/\bar{d}$=(0.078±0.004) 1/Å → $\bar{d}_{(001)}$=(12.8±0.7) Å).

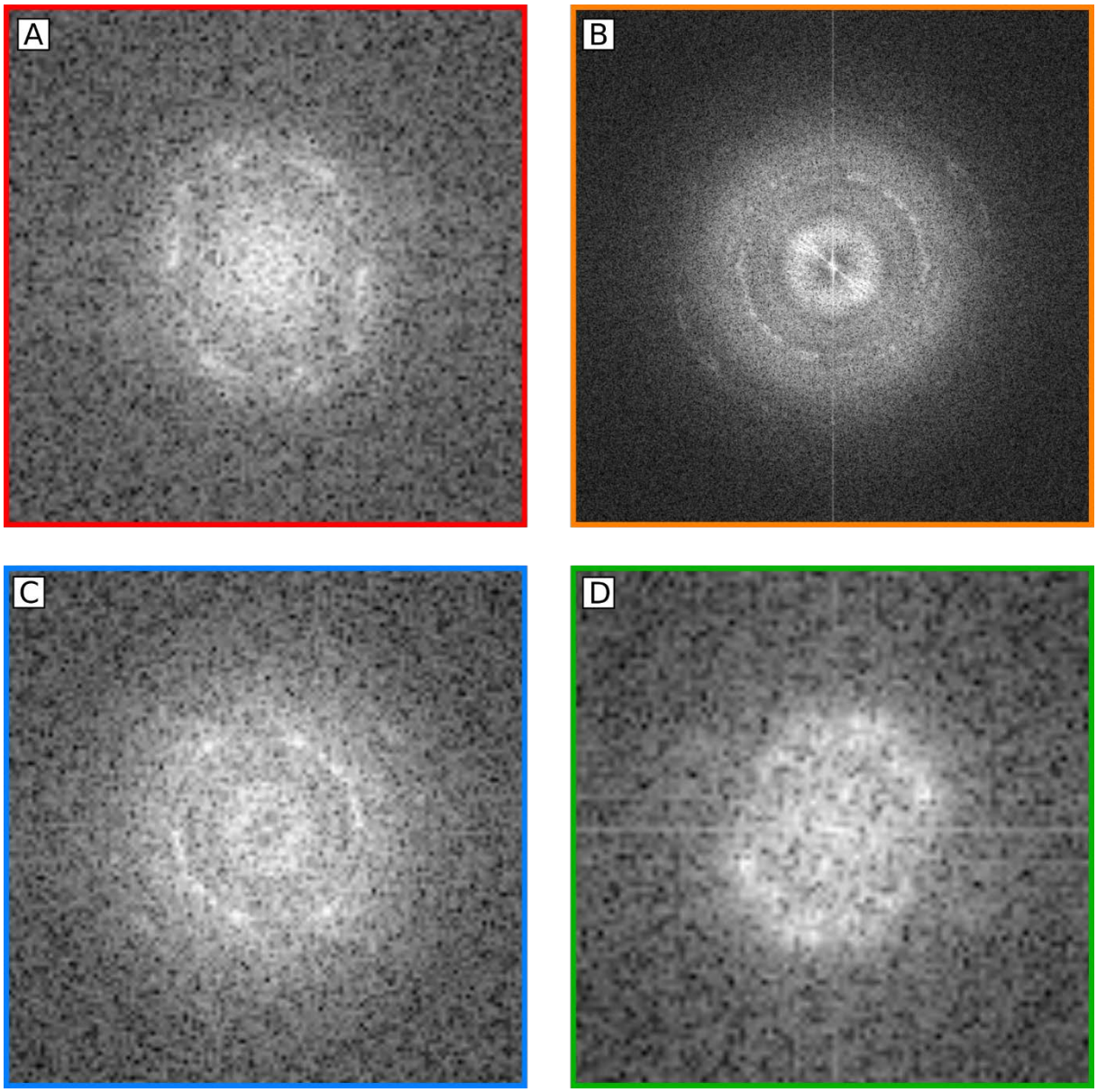

Figure S5. Reduced FFT of HRTEM image from figure 5 A & B in the main text which were used to create the intensity profiles in figure 5 C. A: FFT of small red area in figure 5 A left; B: FFT of figure 5 A right (entire image, orange); C: FFT of small blue are in figure 5 A right; D: FFT of small green area in figure 5 B left.

3. SEM

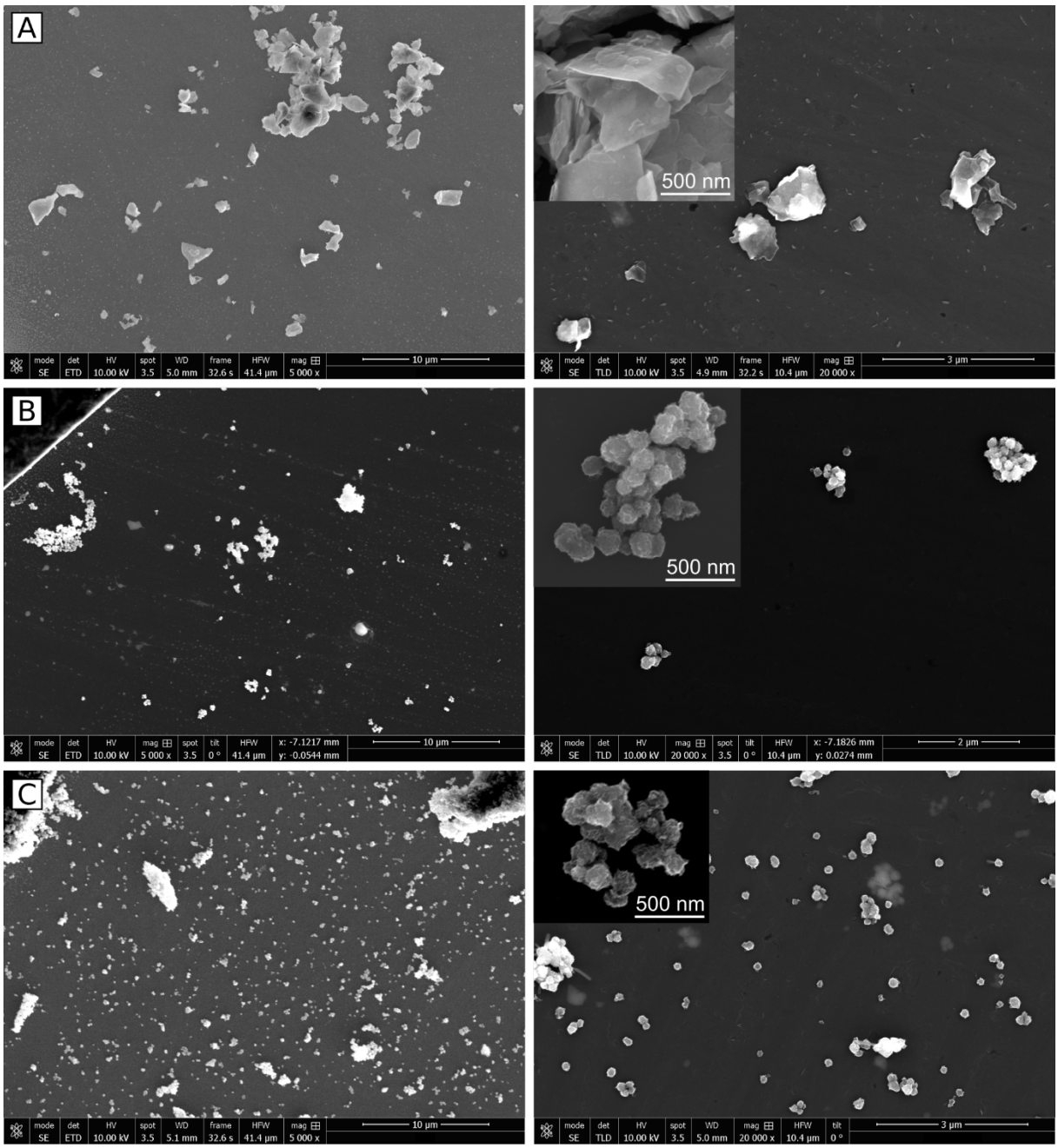

Figure S6. SEM images for particle size and shape analysis of A: MoS_2 powder; B: MoS2.6 powder and C: $MoS_{3.4}$ powder representative for the $MoS_{2+\delta}$ samples in different magnifications. The powders are dispersed on a carbon membrane to separate the particles.

The geometric factor F_G is defined as the increase of the geometric surface area of the electrode after taking particle size and shape into consideration. Figure S6 shows the shape of the particles of the commercial MoS_2 and the synthesized $MoS_{2.6}$ and $MoS_{3.4}$ powder. For the $MoS_{2+\delta}$ particles no difference between the two batches is visible and the shape is approximated with a sphere (r_S: radius) resulting in a surface area of

$$A_{O,S} = 4 \cdot \pi \cdot r_S^2.$$

The MoS_2 particles are approximated with a flattened rotational ellipsoid (r_E: in plane radius, h: height; $r_E > h$):

$$A_{O,E} = 2 \cdot \pi \cdot r_E \left(r_E + \frac{h^2}{\sqrt{r_E^2 - h^2}} \, arsinh\left(\frac{\sqrt{r_E^2 - h^2}}{h} \right) \right)$$

Taking the different projected base areas $A_{C,E/S} = \pi \cdot r^2$ into account, the geometric factor can be described by:

$$F_{G,MoS_2} = \frac{A_{O,E}}{2 \cdot A_{C,E}}, \qquad F_{G,MoS_{2+\delta}} = \frac{A_{O,S}}{2 \cdot A_{C,ES}}$$

With an average diameter of $2 \cdot r_S = (0.18 \pm 0.06)$ µm for $MoS_{2+\delta}$, $2 \cdot r_E = (0.8 \pm 0.9)$ µm and a height of h = 0.04 µm for MoS_2 this results in a geometric factor of

$$F_{G,MoS_2} = 1{,}03 \quad and \quad F_{G,MoS_{2+\delta}} = 2.$$

Thus, the surface of the $MoS_{2+\delta}$ electrode is by factor of ≈1.9 larger than the MoS_2 surface due to particle size and shape.

4. EC

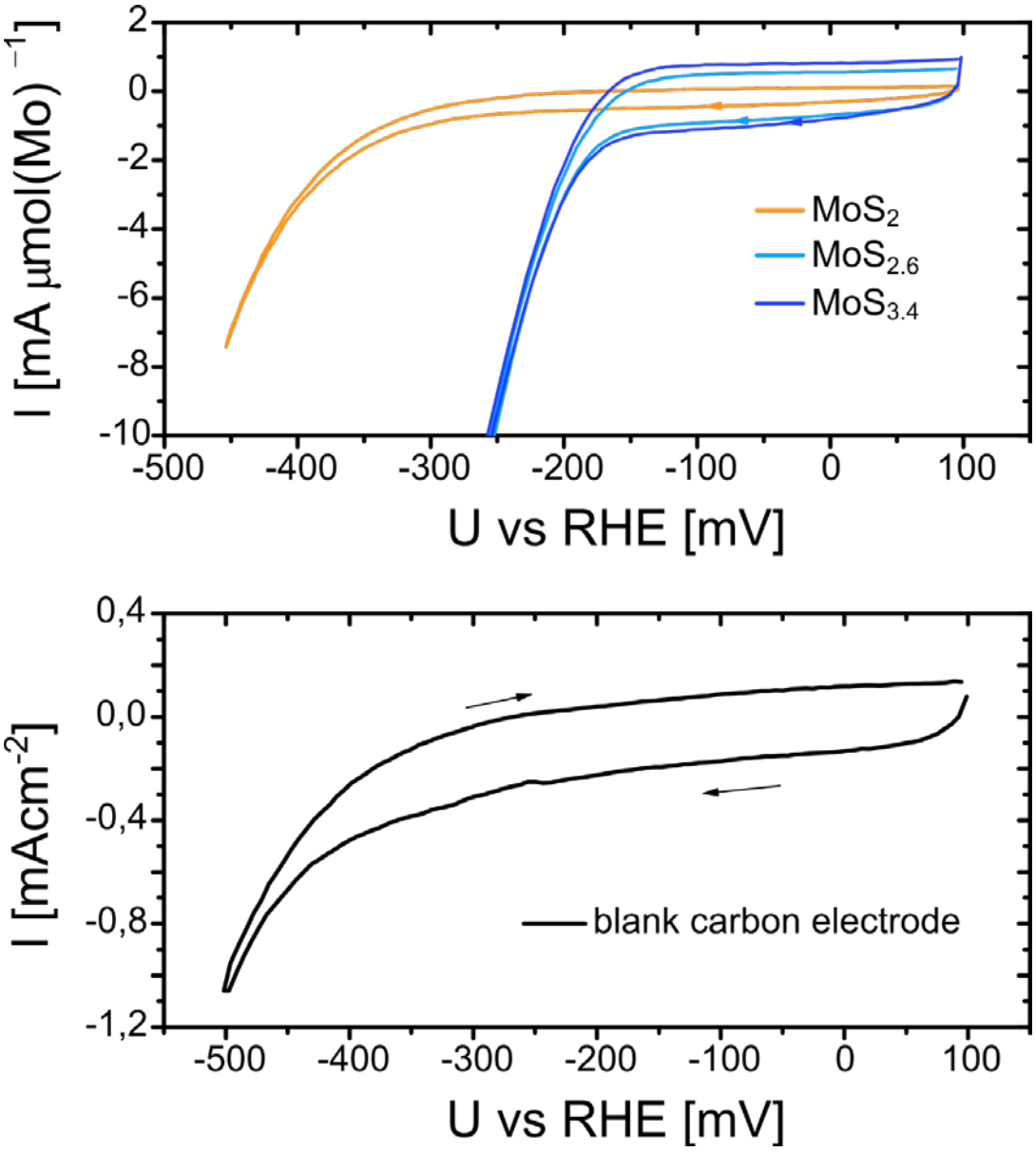

Figure S7. Cyclic voltammetry (cycle 6) in sulfuric acid (0.5 M, pH 0.3) of: *Top:* the two MoS_x samples and MoS_2 normalized to Mo molar concentration (scan rate 20 mV s^{-1}); *Bottom:* The blank carbon electrode.